UNIVERSITY of York

This is a repository copy of *Statistical thermodynamic foundation for mesoscale aggregation in ternary mixtures*.

White Rose Research Online URL for this paper:
https://eprints.whiterose.ac.uk/129733/

Version: Accepted Version

Article:
Shimizu, Seishi orcid.org/0000-0002-7853-1683 and Matubayasi, Nobuyuki (2018) Statistical thermodynamic foundation for mesoscale aggregation in ternary mixtures. Physical Chemistry Chemical Physics. pp. 13777-13784. ISSN 1463-9084

https://doi.org/10.1039/C8CP01207E

Reuse
Items deposited in White Rose Research Online are protected by copyright, with all rights reserved unless indicated otherwise. They may be downloaded and/or printed for private study, or other acts as permitted by national copyright laws. The publisher or other rights holders may allow further reproduction and re-use of the full text version. This is indicated by the licence information on the White Rose Research Online record for the item.

Takedown
If you consider content in White Rose Research Online to be in breach of UK law, please notify us by emailing eprints@whiterose.ac.uk including the URL of the record and the reason for the withdrawal request.

White Rose university consortium
Universities of Leeds, Sheffield & York

eprints@whiterose.ac.uk
https://eprints.whiterose.ac.uk/

Statistical thermodynamic foundation for mesoscale aggregation in ternary mixtures

Seishi Shimizu[1,*] *and Nobuyuki Matubayasi*[2,3]

[1]York Structural Biology Laboratory, Department of Chemistry, University of York, Heslington, York YO10 5DD, United Kingdom.

[2]Division of Chemical Engineering, Graduate School of Engineering Science, Osaka University, Toyonaka, Osaka 560-8531, Japan

[3]Elements Strategy Initiative for Catalysts and Batteries, Kyoto University, Katsura, Kyoto 615-8520, Japan

Corresponding Author: Seishi Shimizu

York Structural Biology Laboratory, Department of Chemistry, University of York, Heslington, York YO10 5DD, United Kingdom.

Tel: +44 1904 328281, Fax: +44 1904 328281, Email: seishi.shimizu@york.ac.uk

ABSTRACT

Ternary solvent mixtures with two mutually miscible and one immiscible solvent pairings often exhibit persistent scattering profiles corresponding to mesoscale structure formation. Despite the morphological information on such mesostructures via extensive scattering measurements and simulation, the origin of these mesostructures, why they persist over a wide composition range, and why they appear around the plait point have remained a mystery. Here we answer all these questions through constructing a fundamental molecular thermodynamic theory, synthetizing thermodynamic stability, scattering and the fluctuation solution theory. The plait point condition, when interpreted via differential geometry, is shown to be the origin of the large structure factor persistent over a wide composition range.

1. Introduction

Long-lived, mesoscale inhomogeneities (aggregates or droplets) have widely been observed in ternary mixtures, which contains two immiscible solvents plus a third component which mixes perfectly with the first two.[1–13] To attain such mesoscale aggregates, whose size can be up to 100 nm, there is no need to look beyond the most commonplace substances, such as water-octanol-ethanol or water-cyclohexane-*tert*-butanol.[1–13] Such mesoscale aggregates (which are also called surfactant-free microemulsions) has attracted much attention recently due to their unusual potential in solubilizing sparingly-soluble substances ("pre-ouzo" or "mesoscale solubilization").[1–13] Mesoscale aggregates have also been reported in important classes of liquids and solubilizers, such as hydrotropes (weakly-amphiphilic solubilizers)[7,11,12,14,15] and ionic liquids,

vastly expanding the types of substances that can be used for solubilization via additional components.[15–22]

Despite its observation in a wide class of solvent mixtures, why mesoscale aggregation takes place in principle has long remained a mystery, despite an extensive morphological characterization of their size, form and composition via X-ray and neutron scattering[3,4,7,8,23] assisted by computer simulation.[8–10,13] Scattering studies have established that the mesoscale aggregates are distinct from critical concentration fluctuation;[3,4,12,13,24] while the critical fluctuations is a featureless change in molecular concentrations, well-defined structural features can be observed for mesoscale aggregates in the structure factors from scattering.[10] Determination of ternary phase diagram has revealed a wide stretch of composition near the plait point (where two binodal curves merge) that give rise to mesoscale fluctuation. [3,4,12,13,24] However, the following questions have remained answered

1. What is the origin of the mesoscale aggregation?
2. Why is it persistent over a wide composition range?
3. Why is it observed near the plait point?

Indeed, decades-long controversy has taken place over all these questions, as has been summarized expertly in recent reviews.[3,4,12,13] The multiplicity of opinions and the lack of consensus evidences the lack of a clear knowledge on the fundamentals of mesoscale aggregation.

To the best of our knowledge, the only attempt to address this question is our recent paper,[25] which, through a combination of thermodynamic stability theory,[26–28] scattering theory[29–31] and elementary differential geometry,[32,33] have shown that

1. the observation of mesoscale aggregation corresponds to the smallness of mixing free energy curvature;[25]
2. the stretch of the mesoscale aggregation region (so-called the pre-ouzo region) signifies the persistence of the small mixing free energy curvature.[25]

Despite these geometrical insights, however, what makes the mixing free energy curvature small has remained unclear, hence the fundamental reason for the existence and persistence of mesostructures and the corresponding scattering intensity have remained a mystery.

This unresolved mystery, as will be shown in Section 2, has arisen from the lack of utilization of the plait point condition,[34–37] around which the persistent mesoscale aggregates have been reported to occur.[1–13] Reformulated fully in the framework of modern differential geometry and linear algebra,[32,33] the plait point condition itself will be shown in Section 2 to be the origin of the smallness of the mixing free energy curvature as well as its persistence, which are the thermodynamic basis for the emergence of the mesoscale aggregates. Such a thermodynamic explanation has to be interpreted microscopically towards a molecular-based understanding of the structure and interaction of the mesoscale aggregates. Hence, we furnish in Section 3 a theoretical framework that can readily be exploited to extract the interactions between each molecular species (quantified via Kirkwood-Buff integrals (KBIs)[38–49]) based on mixing free energy data when made available, and conversely to gain some information on mixing free energy from the inter-species KBIs. KBIs have previously been used to characterize micro-heterogeneity in microemulsions.[45–47] In view of the utmost present challenge in accurately interpreting scattering profiles, the theoretical link furnished in Section 3 is intended chiefly for paving a way theoretically towards a molecular-based elucidation that should emerge with the availability of more experimental data.

2. Plait point condition and mixing free energy

Consider a ternary mixture consisting of water ($i = 1$), solute ($i = 2$) and hydrotrope ($i = 3$) under a constant temperature T and the pressure P. Under this condition, let $G^{mix}(N_1, N_2, N_3)$ be the mixing free energy of mixing N_1 water, N_2 solute and N_3 hydrotrope molecules. Let us introduce the normalized mixing free energy, $g = \frac{G^{mix}}{N}$, where $N = N_1 + N_2 + N_3$ is the total number of molecules.[25,26,28] Due to the relationship between the mole fractions (x_i for the species i), $x_1 + x_2 + x_3 = 1$, we choose x_2 and x_3 as independent variables, so that g is the function only of x_2 and x_3, i.e., $g(x_2, x_3)$. Following the classical chemical thermodynamics of phase stability, we postulate that $g(x_2, x_3)$ is analytic.[26,27] This normalized mixing free energy has a direct link[25,28] to the concentration-concentration structure factor[29–31] measurable by scattering experiments.[50]

Our goal is to clarify the geometrical properties of a surface, $z = g(x_2, x_2)$ in relation to the fluctuation and scattering around the point. To this end, let us consider the tie line and its two end points A and B (Figure 1), whose coordinates are (x_{2A}, x_{3A}) and (x_{2B}, x_{3B}).[51] A schematic diagram plotting g along AB can be found in Figure 2. A plane, which contains the tie line, can be tangent to $z = g(x_2, x_3)$ at both points, which means that the point (x_{2B}, x_{3B}) is on a plane which is tangent to $z = g(x_2, x_3)$ at (x_{2A}, x_{3A}). This can be expressed as[51]

$$g(x_{2B}, x_{3B}) = g(x_{2A}, x_{3A}) + \left.\frac{\partial g}{\partial x_2}\right|_A (x_{2B} - x_{2A}) + \left.\frac{\partial g}{\partial x_3}\right|_A (x_{3B} - x_{3A}) \quad (1)$$

under the condition that

$$g_2 \equiv \left.\frac{\partial g}{\partial x_2}\right|_A = \left.\frac{\partial g}{\partial x_2}\right|_B \qquad g_3 \equiv \left.\frac{\partial g}{\partial x_3}\right|_A = \left.\frac{\partial g}{\partial x_3}\right|_B \quad (2)$$

Thus the coordinates (x_{2A}, x_{3A}) and (x_{2B}, x_{3B}) can be varied continuously to generate a number of tie lines between them. When two such points merge, namely, $(x_{2B}, x_{3B}) \rightarrow (x_{2A}, x_{3A})$, the merged point is called the plait point (Figures 1 and 2). Around this point, we introduce $dx_2 = x_{2B} - x_{2A}$ and $dx_3 = x_{3B} - x_{3A}$ for convenience, and rewrite Eqs. (1) and (2) into the following compact form

$$g(x_{2A} + dx_2, x_{3A} + dx_3) - g(x_{2A}, x_{3A}) = g_2 dx_2 + g_3 dx_3 \quad (3)$$

It should be noted that Eq. (3) holds at any orders of dx_2 and dx_3 in the progression to the plait point. Accordingly, the expansion of the l.h.s of Eq. (3) up to the second order yields

$$\sum_{i,j} g_{ij} dx_i dx_j = 0 \quad (4)$$

where $\boldsymbol{g} = (g_{ij}) \equiv \left(\frac{\partial^2 g}{\partial x_i \partial x_j}\Big|_A \right)$. Eq. (4) is in fact a quadratic form[33]

$$(dx_2\ dx_3) \begin{pmatrix} g_{22} & g_{23} \\ g_{23} & g_{33} \end{pmatrix} \begin{pmatrix} dx_2 \\ dx_3 \end{pmatrix} = 0 \quad (5)$$

whose geometrical interpretation is that the vector $\boldsymbol{g} \begin{pmatrix} dx_2 \\ dx_3 \end{pmatrix}$ is perpendicular to $\begin{pmatrix} dx_2 \\ dx_3 \end{pmatrix}$. (It is easy to see that $\boldsymbol{g} \begin{pmatrix} dx_2 \\ dx_3 \end{pmatrix}$ cannot be a non-zero vector; if it is null, $\boldsymbol{g} \propto \begin{pmatrix} 0 & 1 \\ -1 & 0 \end{pmatrix}$ in contradiction to the matrix symmetry.) Hence the vector we seek is a null vector,

$$\begin{pmatrix} g_{22} & g_{23} \\ g_{23} & g_{33} \end{pmatrix} \begin{pmatrix} dx_2 \\ dx_3 \end{pmatrix} = \begin{pmatrix} 0 \\ 0 \end{pmatrix} \quad (6)$$

and in order that for Eq. (6) to have a non-trivial solution

$$\Gamma \equiv \begin{vmatrix} g_{22} & g_{23} \\ g_{23} & g_{33} \end{vmatrix} = 0 \quad (7)$$

must be fulfilled.[33] (As will later be explained, this Γ plays a central role in thermodynamic stability and has a direct link to the structure factor. See Appendix A.)

Note that Eq. (7) is in fact the spinodal condition, which means that at the plait point the binodal and spinodal points converge. Hence, noting that Eq. (7) has been derived at the point A yet the symmetry requires that the same condition be fulfilled also at point B as well, Γ should remain constant under the (infinitesimal) displacement (dx_2, dx_3)

$$d\Gamma = \frac{\partial \Gamma}{\partial x_2} dx_2 + \frac{\partial \Gamma}{\partial x_3} dx_3 = 0 \tag{8}$$

Eqs. (6) and (8) in combination yields

$$\begin{pmatrix} g_{22} & g_{23} \\ g_{23} & g_{33} \\ \frac{\partial \Gamma}{\partial x_2} & \frac{\partial \Gamma}{\partial x_3} \end{pmatrix} \begin{pmatrix} dx_2 \\ dx_3 \end{pmatrix} = \begin{pmatrix} 0 \\ 0 \\ 0 \end{pmatrix} \tag{9}$$

For Eq. (9) to have non-trivial solutions, cofactors of the matrix therein must be zero,[33] which leads to the following plait-point condition:

$$\begin{vmatrix} g_{23} & g_{33} \\ \frac{\partial \Gamma}{\partial x_2} & \frac{\partial \Gamma}{\partial x_3} \end{vmatrix} = 0 \tag{10}$$

Eq. (10) has originally been derived by Gibbs,[52] and has subsequently been given rigorous mathematical derivations.[51,53–55] However, our re-derivation, based on a full exploitation of linear algebra, is to the best of our knowledge much simpler. This plait-point condition is well-known and has been applied to a number of questions in chemical engineering.[34,36,37]

Now we aim to establish a link between the plait point condition (Eqs. (7) and (10)) to elucidate the origin of mesoscale fluctuations in ternary mixtures, which has been observed around the plait point. To this end, building on our previous paper based only on Eq. (7),[25] we employ the rudiments of differential geometry.[32,33] We have previously shown that the zero Hessian (Eq. (7)) means that one of the principal curvatures of $g(x_2, x_3)$ is zero at the point.[25] In addition, it can be shown easily

that the principal direction with zero curvature is along the limiting tie line AB, for the change of Γ is zero along this direction according to Eq. (8).

Let us now take a ξ_1 axis along the direction corresponding to the smaller curvature, and a ξ_2 axis perpendicular to ξ_1. (In Figure 1, the ξ_1 axis is parallel to the tie line at the plait point; in Figure 2 the horizontal axis is the ξ_1 axis). Let the curvatures of $g(x_2, x_3)$ κ_1 and κ_2 along these axes, respectively (κ_1 = 0 at the plait point). Such a coordinate system (ξ_1, ξ_2) is proven to be orthogonal[32,33] and will be helpful in interpreting the plait point condition (Eq. (10)), which can be rewritten as

$$\begin{vmatrix} g'_{12} & g'_{22} \\ \frac{\partial \Gamma}{\partial \xi_1} & \frac{\partial \Gamma}{\partial \xi_2} \end{vmatrix} = 0 \tag{11}$$

where $g'_{ij} \equiv \left.\frac{\partial^2 g}{\partial \xi_i \partial \xi_j}\right|_A$. Since $g'_{12} = 0$ for off-diagonal elements but $g'_{22} \neq 0$, Eq. (11) yields the following simple relationship:

$$\frac{\partial \Gamma}{\partial \xi_1} = 0 \tag{12}$$

Thus at the plait point not only $\Gamma = 0$ but also its change along the ξ_1 axis is zero, namely, $\frac{\partial \Gamma}{\partial \xi_1} = 0$. This means, taken together with the analytic nature of $g(\xi_1, \xi_2)$, that the smallness of Γ persists around the plait point, because its increment along the ξ_1 axis is also zero.

Now we move off the plait point to its surroundings where $\Gamma \neq 0$ yet due to Eq. (12) is nevertheless very small, namely

$$\Gamma = \begin{vmatrix} g_{22} & g_{23} \\ g_{23} & g_{33} \end{vmatrix} \simeq 0 \tag{13}$$

$$\begin{vmatrix} g_{23} & g_{33} \\ \frac{\partial \Gamma}{\partial x_2} & \frac{\partial \Gamma}{\partial x_3} \end{vmatrix} \simeq 0 \tag{14}$$

Note that the determinants in Eqs. (13) and (14), albeit small, are not zero, hence Γ can now be diagonalized through an appropriate transformation of coordinates,[32,33] $(x_2, x_3) \rightarrow (\xi_1, \xi_2)$, via rotation, as

$$\Gamma = \begin{vmatrix} g'_{11} & 0 \\ 0 & g'_{22} \end{vmatrix} = \kappa_1 \kappa_2 \simeq 0 \tag{15}$$

$$\begin{vmatrix} \frac{\partial \Gamma}{\partial \xi_1} & \frac{\partial \Gamma}{\partial \xi_2} \\ 0 & g'_{22} \end{vmatrix} \simeq 0 \tag{16}$$

where ξ_1 and ξ_2 correspond to the directions for minimum and maximum curvatures κ_1 and κ_2, respectively. From Eqs. (15) and (16), it follows that

$$\frac{\partial \Gamma}{\partial \xi_1} \kappa_2 \simeq 0 \tag{17}$$

Since κ_2, the maximum curvature, is non-zero and is not vanishingly small, we obtain

$$\Gamma \simeq 0 \tag{18}$$

$$\frac{\partial \Gamma}{\partial \xi_1} \simeq 0 \tag{19}$$

Hence Γ is small and the increment of Γ along the ξ_1 axis is still very small, meaning that Γ is persistently small along the ξ_1 axis. The focus on this principle direction enabled by differential geometry facilitates the argument through the reduced dimensionality (Figure 2) regardless of the number of components.

We have thus proven that, due to the continuity of the mixing free energy function, Γ is close to zero around the plait point, and its increment is also close to zero. Here we discuss the ramification of Eqs. (18) and (19) using the properties of Γ[25] (see Appendix A for the background information).

1. Thermodynamic stability is governed by the stability function $\Psi = \frac{x_2 x_3}{(k_B T)^2}\Gamma$.[25–27]
2. The stability function is inversely proportional to the concentration-concentration structure factor at $q = 0$, $S_{CC}(0)$, via $\Psi = \frac{x_2 x_3}{S_{CC}(0)}$.[25,29–31]
3. From 1 and 2, Γ is inversely proportional to $S_{CC}(0)$.[25,28]
4. From 3 and Eqs. (18) and (19), a persistently small Γ along the ξ_1 axis is equivalent to a persistently large $S_{CC}(0)$ along the ξ_1 axis.
5. Due to the continuity of the function $S_{CC}(q)$, $S_{cc}(q)$ is persistently large at small q along the ξ_1 axis.[25]

Thus we have proven that the plait point condition is the cause of a persistently large structure factor at small q observed in ternary fluid mixtures, which has been referred to as mesoscale solubilization or the pre-ouzo effect. [1–13]

3. Linking the mixing free energy surface to KBIs

The chief aim of this section is to furnish the theoretical foundation for elucidating the molecular basis for the persistently small mixing free energy curvature, i.e., to pave a way towards the future understanding with the expansion in the availability of experimental data. Indeed, what has made the study of mesoscale fluctuations particularly challenging, and even its existence a matter of controversy, is the difficulty of separating them from the critical fluctuation, even though accumulating evidence show that mesoscale fluctuation is distinct from critical fluctuation.[10] This difficulty would be a stumbling block in the evaluation of the KBIs (Kirkwood-Buff integrals) that characterize the long-range solution fluctuation.[1–13] Here we establish a link between KBIs and the mixing free energy curvature, with a view that the directional information on mixing free energy

curvature, in combination with the approximate location of the plait point, would be helpful in uncovering additional information on the solution structure, through a comparison between the KBIs and the phase diagram.

The KBIs and the chemical potential μ_i of species i obeys the following relationships:[38,40,49,56–58]

$$A_{ij} \equiv \frac{V}{kT}\left(\frac{\partial \mu_i}{\partial N_j}\right)_{T,V,N_{j'}} = \frac{V}{kT}\left(\frac{\partial \mu_i}{\partial N_j}\right)_{T,P,N_j'} + \frac{V_i V_j}{kT\kappa_T} \tag{20}$$

$$B_{ij} \equiv \frac{kT}{V}\left(\frac{\partial N_i}{\partial \mu_j}\right)_{T,V,\mu_j'} = \rho_i \rho_j G_{ij} + \rho_i \delta_{ij} \tag{21}$$

$$AB = E \tag{22}$$

where E is a unit matrix, V is the volume of the system, k is the Boltzmannn constant, V_i is the partial molar volume of the species i, and and κ_T is the isothermal compressibility of the solution. G_{ij} is the KBI between species i and j, defined in terms of the ensemble average $\langle\ \rangle$ involving N_i (the number of molecules of the species i) as $G_{ij} = V\left[\frac{\langle N_i N_j\rangle - \langle N_i\rangle\langle N_j\rangle}{\langle N_i\rangle\langle N_j\rangle} - \frac{\delta_{ij}}{\langle N_i\rangle}\right]$, where δ_{ij} is Kronecker's delta. The matrix A is accessible via experiments, while the matrix B, which is related to KBIs, can be obtained via the matrix inversion (Eq. (22)).[40,49,57] Note that Eqs (20)-(22) are based only on the fundamental principles of classical statistical thermodynamics; no further assumptions has been made other than the classical nature of the molecules.[40,59]

Since isothermal compressibility diverges near the plait point[60], the second term in Eq. (20) should be negligible, which leads to the following approximation:

$$A_{ij} \simeq \frac{V}{kT}\left(\frac{\partial \mu_i}{\partial N_j}\right)_{T,P,N_j'} \equiv \frac{V}{kT}\mu_{ij} \tag{23}$$

This divergence of isothermal compressibility is evidenced by the experimentally-observed divergent scattering intensity at $q \to 0$, indicating a divergent structure factor[1–13], when combined with a rigorous relationship between the structure factor and isothermal compressibility valid even for multiple-component solution.[61,62] Hence linking KBIs with the Hessian of the normalized mixing free energy is now reduced to the variable transformation between (N_1, N_2, N_3) and (x_2, x_3, N), for which the following Jacobians will play a crucial role:[33,63]

$$\frac{\partial(N_1,N_2,N_3)}{\partial(x_2,x_3,N)} = \begin{pmatrix} -N & N & 0 \\ -N & 0 & N \\ 1-x_2-x_3 & x_2 & x_3 \end{pmatrix} \tag{24}$$

$$\frac{\partial(x_2,x_3,N)}{\partial(N_1,N_2,N_3)} = \frac{1}{N}\begin{pmatrix} -x_2 & -x_3 & N \\ 1-x_2 & -x_3 & N \\ -x_2 & 1-x_3 & N \end{pmatrix} \tag{25}$$

Note that $\frac{\partial(N_1,N_2,N_3)}{\partial(x_2,x_3,N)}\frac{\partial(x_2,x_3,N)}{\partial(N_1,N_2,N_3)} = E$ can easily be proven.

Firstly, we express g_{ij} in terms of the matrix $\boldsymbol{\mu} = (\mu_{ij})$ in Eq. (23). Using Eq. (24) and some useful relationships obtainable upon first-order differentiation (Appendix B), we obtain the following compact result

$$g_{ij} = N v_j^T \boldsymbol{\mu} v_i \tag{26}$$

where v_i are defined as

$$v_2 = \begin{pmatrix} 1 \\ -1 \\ 0 \end{pmatrix} \quad v_3 = \begin{pmatrix} 1 \\ 0 \\ -1 \end{pmatrix} \tag{27}$$

This means that when KBIs between all the three species are determinable via Faber-Ziman partial structure factors at the $q \to 0$ limit,[50] the inverse of the KBIs, namely $\boldsymbol{\mu}$ via Eq. (23), can yield the Hessian of the normalized mixing free energy, thereby providing useful information on the mixing free energy surface.

Secondly, we establish a route to KBIs from the mixing free energy Hessian using Eq. (25). By virtue of the useful first-order differentiation results in Appendix B, we obtain the following compact results

$$N\mu_{ij} = u_j^T \boldsymbol{g} u_i \tag{28}$$

where

$$u_1 = \begin{pmatrix} -x_2 \\ -x_3 \end{pmatrix} \qquad u_2 = \begin{pmatrix} 1 - x_2 \\ -x_3 \end{pmatrix} \qquad u_3 = \begin{pmatrix} -x_2 \\ 1 - x_3 \end{pmatrix} \tag{29}$$

This means that the local curvature information on $g(x_2, x_3)$ can directly be used as an input for the KBIs.

We have thus obtained the direct relationships that link $\boldsymbol{g}$ to $\boldsymbol{\mu}$ and $\boldsymbol{\mu}$ to $\boldsymbol{g}$. Noting that $\boldsymbol{\mu}$ is the inverse matrix of the KBIs, we conclude that two-way translation between the KBIs and the mixing free energy curvature has been established, which will link the phase diagram and scattering approaches to mesoscale fluctuations. At present, there is no experimental dataset available in the literature that could be used to evaluate the KBIs; to this end, extensive mixing free energy measurements should be conducted. Likewise, determining KBIs from simulation is still a challenging problem even for simple fluid mixtures, for which an efficient approach is actively investigated.[64] Nevertheless, the significance of the theory here is in the unification of fluctuation-based and curvature-based perspectives in the understanding of mixing inhomogeneities.

4. Conclusion

Simple ternary mixtures that consist of two miscible and one immiscible pairs of solvents often exhibit anomalous and persistent scattering profiles corresponding to mesoscale structures.[1–13] Extensive scattering measurements, conducted over the last few decades, are revealing the morphology of the aggregates and droplets within the solution,[3,4,7,8,23] and computer simulations are providing insights into the subtle balance of forces that leads to such structures.[8–10,13] However, the fundamental questions remained unaddressed. What is the origin of these mesostructures? Why do they persist over a wide composition range? Why do they appear around the plait point?

This paper provided a clear answer to these questions, combining the insights from the thermodynamic theory of phase stability,[26–28] elementary differential geometry,[32,33] scattering theory[29–31] and statistical thermodynamics of fluctuation.[38–40,43,44,48] Through a simple re-derivation of plait point condition by exploiting the fundamental properties of linear space and differential geometry,[32,33,63] we have shown that the behaviour of mixing free energy around the plait point inevitably leads not only to the zero curvature of the mixing free energy surface along a principal direction but also to a zero derivative of curvature along the same axis, leading to a persistently small free energy curvature. Since the concentration-concentration structure factor is inversely proportional to this curvature,[25] our finding have thus revealed the origin of the strong and persistent scattering intensity coming from this region in the phase diagram.

In addition, in view of the difficulty in the characterization of aggregate and droplet structures solely from scattering, we have provided a general theoretical framework upon which mixing free energy information can directly be linked to the Kirkwood-Buff integrals that quantify the potential of mean force interactions between each species.[38–40,43,44,48] This new link will generalize our

earlier theory of hydrotropy in its link between solubilization and scattering[15–22,25] and will hopefully provide a complementary route to the elucidation of mesostructures.

Appendix A

Here we briefly summarize the background knowledge on the relationship between thermodynamic stability, structure factor and curvature. Let $g_{mix}(x_2, x_3, \dots, x_M)$ be the free energy of mixing in the *M*-component system, where x_i is the mole-fraction of the component i. Note that there are only $M-1$ variables due to $\sum_i x_i = 1$. Gazzillo[28] defined the following matrix

$$g_{ij} = \left(\frac{\partial g^{mix}}{\partial x_i \partial x_j}\right)_{T,\rho_k} \qquad \text{for } i \geq 2, j \geq 2 \tag{A1}$$

and the following stability function via the Hessian determinant, $\Gamma = \det g$ (Eq. (7)), as

$$\Psi = \frac{\prod_i x_i}{(k_B T)^{M-1}} \Gamma \tag{A2}$$

The phase stability condition for the mixture, using Eq, (A2), is $\Psi > 0$; spinodal line is the collection of points $(x_2, \dots, x_M)$ that satisfy $\Psi(x_2, \dots, x_M) = 0$.[28] Gazillo has shown that the stability function Ψ can be related to the concentration-concentration structure factor at $q = 0$, $S_{CC}(0)$, as[28]

$$\Psi = \frac{\prod_i x_i}{S_{CC}(0)} \tag{A3}$$

Based on Eqs. (A3) and (A4), $S_{CC}(0)$ and Γ has the following reciprocal relationship:

$$S_{CC}(0) = \frac{(k_B T)^{M-1}}{\Gamma} \tag{A4}$$

In our previous paper,[25] we have gone so far as to show that the Hessian determinant Γ can be expressed as the product of its principal curvatures, α_i along the principal axes[32], such that

$$S_{CC}(0) = \frac{(k_B T)^{M-1}}{\prod \alpha_i} \tag{A5}$$

Thus the divergence of $S_{CC}(0)$ at a given composition comes from at least one of the principal curvatures being close to zero. Yet what makes the curvature so small has not been identified in our previous paper, but has been linked directly to the plait point condition in this paper (Section 2).

Appendix B

Here we derive Eqs. (26)-(29). To do so, we will present some useful relationships for linking the mixing free energy Hessian to KBIs. Throughout the derivation here, the variables T and P have been omitted.

Our first goal is to derive Eqs. (26) and (27). To do so, we must start from the first order derivatives of μ_i with respect to the mole fractions. Using the Jacobian,[33,63] we have

$$\begin{pmatrix} \frac{\partial G}{\partial x_2} \\ \frac{\partial G}{\partial x_3} \\ \frac{\partial G}{\partial N} \end{pmatrix} = \begin{pmatrix} -N & N & 0 \\ -N & 0 & N \\ 1-x_2-x_3 & x_2 & x_3 \end{pmatrix} \begin{pmatrix} \frac{\partial G}{\partial N_1} \\ \frac{\partial G}{\partial N_2} \\ \frac{\partial G}{\partial N_3} \end{pmatrix} \tag{B1}$$

Noting that $\mu_i = \left(\frac{\partial G}{\partial N_i}\right)$ and $G = Ng(x_2, x_3)$, Eq. (B1) can be rewritten as

$$\frac{\partial g}{\partial x_2} = \mu_2 - \mu_1 \tag{B2}$$

$$\frac{\partial g}{\partial x_3} = \mu_3 - \mu_1 \tag{B3}$$

$$g = x_2\mu_2 + x_3\mu_3 + (1-x_2-x_3)\mu_1 \tag{B4}$$

We have thus established the first order derivatives of g with respect to x_2 and x_3 via Eqs. (B2) and (B3).

We then calculate g_{ij}, i.e., the second order derivatives of g with respect to x_2 and x_3. using the same Jacobian (Eq. (24)). To this end, combining Eqs. (B2), (B3) and (24) yields

$$\frac{\partial^2 g}{\partial x_2^2} = \frac{\partial(\mu_2 - \mu_1)}{\partial x_2} = -N(\mu_{21} - \mu_{11}) + N(\mu_{22} - \mu_{21}) \tag{B5}$$

$$\frac{\partial^2 g}{\partial x_2 \partial x_3} = \frac{\partial(\mu_2 - \mu_1)}{\partial x_3} = -N(\mu_{21} - \mu_{11}) + N(\mu_{32} - \mu_{31}) \tag{B6}$$

$$\frac{\partial^2 g}{\partial x_3^2} = \frac{\partial(\mu_3 - \mu_1)}{\partial x_3} = -N(\mu_{31} - \mu_{11}) + N(\mu_{33} - \mu_{13}) \tag{B7}$$

Simple yet tedious algebra shows that Eqs. (B5)-(B7) can be expressed in a more compact manner summarized by Eqs. (26) and (27).

Our second goal is to derive Eqs. (28) and (29). The Jacobian of Eq. (25) yields the following useful relationship between the chemical potential and the first-order derivative of $g(x_2, x_3)$ as

$$\begin{pmatrix} \frac{\partial G}{\partial N_1} \\ \frac{\partial G}{\partial N_2} \\ \frac{\partial G}{\partial N_3} \end{pmatrix} = \frac{1}{N} \begin{pmatrix} -x_2 & -x_3 & N \\ 1 - x_2 & -x_3 & N \\ -x_2 & 1 - x_3 & N \end{pmatrix} \begin{pmatrix} \frac{\partial G}{\partial x_2} \\ \frac{\partial G}{\partial x_3} \\ \frac{\partial G}{\partial N} \end{pmatrix} \tag{B8}$$

Noting again that $\mu_i = \left(\frac{\partial G}{\partial N_i}\right)$ and $G = Ng(x_2, x_3)$, we obtain

$$\mu_1 = -x_2 g_2 - x_3 g_3 + g \tag{B9}$$

$$\mu_2 = (1 - x_2) g_2 - x_3 g_3 + g \tag{B10}$$

$$\mu_3 = -x_2 g_2 + (1 - x_3) g_3 + g \tag{B11}$$

Now we differentiate Eqs. (B9)-(B11) once more with respect to N_1, N_2 and N_3. The derivative with respect to N_i is transformed to those with respect to x_2, x_3 and N via the Jacobian (Eq. (25)). Note that the following relationships (for $j = 2,3$) will play the key role in the derivation:

$$\frac{\partial \mu_1}{\partial x_j} = -x_2 g_{2j} - x_3 g_{3j} \tag{B12}$$

$$\frac{\partial \mu_2}{\partial x_j} = (1 - x_2) g_{2j} - x_3 g_{3j} \tag{B13}$$

$$\frac{\partial \mu_3}{\partial x_j} = -x_2 g_{2j} + (1 - x_3) g_{3j} \tag{B14}$$

The derivation of Eq. (28) requires a tedious algebra. Using Eq. (25) for the differentiation of μ_1, and with the help of Eqs. (B12)-(B14), we obtain

$$\begin{pmatrix} \mu_{11} \\ \mu_{12} \\ \mu_{13} \end{pmatrix} = \begin{pmatrix} \frac{\partial \mu_1}{\partial N_1} \\ \frac{\partial \mu_1}{\partial N_2} \\ \frac{\partial \mu_1}{\partial N_3} \end{pmatrix} = \frac{1}{N} \begin{pmatrix} -x_2 & -x_3 & N \\ 1 - x_2 & -x_3 & N \\ -x_2 & 1 - x_3 & N \end{pmatrix} \begin{pmatrix} -x_2 g_{22} - x_3 g_{32} \\ -x_2 g_{23} - x_3 g_{33} \\ 0 \end{pmatrix} \tag{B15}$$

$$\begin{pmatrix} \mu_{21} \\ \mu_{22} \\ \mu_{23} \end{pmatrix} = \begin{pmatrix} \frac{\partial \mu_2}{\partial N_1} \\ \frac{\partial \mu_2}{\partial N_2} \\ \frac{\partial \mu_2}{\partial N_3} \end{pmatrix} = \frac{1}{N} \begin{pmatrix} -x_2 & -x_3 & N \\ 1 - x_2 & -x_3 & N \\ -x_2 & 1 - x_3 & N \end{pmatrix} \begin{pmatrix} (1 - x_2) g_{22} - x_3 g_{32} \\ (1 - x_2) g_{23} - x_3 g_{33} \\ 0 \end{pmatrix} \tag{B16}$$

$$\begin{pmatrix} \mu_{31} \\ \mu_{32} \\ \mu_{33} \end{pmatrix} = \begin{pmatrix} \frac{\partial \mu_2}{\partial N_1} \\ \frac{\partial \mu_2}{\partial N_2} \\ \frac{\partial \mu_2}{\partial N_3} \end{pmatrix} = \frac{1}{N} \begin{pmatrix} -x_2 & -x_3 & N \\ 1 - x_2 & -x_3 & N \\ -x_2 & 1 - x_3 & N \end{pmatrix} \begin{pmatrix} -x_2 g_{22} + (1 - x_3) g_{32} \\ -x_2 g_{23} + (1 - x_3) g_{33} \\ 0 \end{pmatrix} \tag{B17}$$

Through straightforward yet tedious algebra, Eqs. (B15)-(B17) can be shown to be summarized compactly by Eqs. (28) and (29).

Acknowledgements

We thank Steven Abbott and Tom Nicol for a careful reading of the manuscript. This work was supported by the Gen Foundation (to S.S.), by Grants-in-Aid for Scientific Research (Nos. 15K13550 and 26240045) from the Japan Society for the Promotion of Science (to N.M.), and the

Elements Strategy Initiative for Catalysts and Batteries and the Post-K Supercomputing Project from the Ministry of Education, Culture, Sports, Science, and Technology (to N.M.).

References

1 D. Subramanian, D. A. Ivanov, I. K. Yudin, M. A. Anisimov and J. V. Sengers, *J. Chem. Eng. Data*, 2011, **56**, 1238–1248.

2 D. Subramanian and M. A. Anisimov, *J. Phys. Chem. B*, 2011, **115**, 9179–9183.

3 D. Subramanian, C. T. Boughter, J. B. Klauda, B. Hammouda and M. A. Anisimov, *Faraday Discuss.*, 2013, **167**, 217–238.

4 D. Subramanian, J. B. Klauda, P. J. Collings and M. A. Anisimov, *J. Phys. Chem. B*, 2014, **118**, 5994–6006.

5 D. Subramanian and M. A. Anisimov, *Fluid Phase Equilib.*, 2014, **362**, 170–176.

6 A. E. Robertson, D. H. Phan, J. E. Macaluso, V. N. Kuryakov, E. V. Jouravleva, C. E. Bertrand, I. K. Yudin and M. A. Anisimov, *Fluid Phase Equilib.*, 2015, **407**, 243–254.

7 O. Diat, M. L. Klossek, D. Touraud, B. Deme, I. Grillo, W. Kunz and T. Zemb, *J. Appl. Crystallogr.*, 2013, **46**, 1665–1669.

8 S. Schöttl, D. Touraud, W. Kunz, T. Zemb and D. Horinek, *Colloids Surfaces A Physicochem. Eng. Asp.*, 2015, **480**, 222–227.

9 S. Schöttl, J. Marcus, O. Diat, D. Touraud, W. Kunz, T. Zemb and D. Horinek, *Chem. Sci.*, 2014, **5**, 2909–3340.

10 T. N. Zemb, M. Klossek, T. Lopian, J. Marcus, S. Schöettl, D. Horinek, S. F. Prevost, D. Touraud, O. Diat, S. Marčelja and W. Kunz, *Proc. Natl. Acad. Sci. U. S. A.*, 2016, **113**, 4260–4265.

11 T. Buchecker, S. Krickl, R. Winkler, I. Grillo, P. Bauduin, D. Touraud, A. Pfitzner and W. Kunz, *Phys. Chem. Chem. Phys.*, 2016, **19**, 1806–1816.

12 W. Kunz, K. Holmberg and T. Zemb, *Curr. Opin. Colloid Interface Sci.*, 2016, **22**, 99–107.

13 S. Schöttl and D. Horinek, *Curr. Opin. Colloid Interface Sci.*, 2016, **22**, 8–13.

14 P. Bauduin, F. Testard and T. Zemb, *J. Phys. Chem. B*, 2008, **112**, 12354–12360.

15 S. Shimizu and N. Matubayasi, *Phys. Chem. Chem. Phys.*, 2017, **19**, 23597–23605.

16 J. J. Booth, S. Abbott and S. Shimizu, *J. Phys. Chem. B*, 2012, **116**, 14915–14921.

17 S. Shimizu, J. J. Booth and S. Abbott, *Phys. Chem. Chem. Phys.*, 2013, **15**, 20625–20632.

18 S. Shimizu and N. Matubayasi, *J. Phys. Chem. B*, 2014, **118**, 10515–10524.

19 J. J. Booth, M. Omar, S. Abbott and S. Shimizu, *Phys Chem Chem Phys*, 2015, **17**, 8028–8037.

20 S. Shimizu and N. Matubayasi, *Phys. Chem. Chem. Phys.*, 2016, **18**, 25621–25628.

21 T. W. J. Nicol, N. Matubayasi and S. Shimizu, *Phys. Chem. Chem. Phys.*, 2016, **18**, 15205–15217.

22 S. Abbott, J. J. Booth and S. Shimizu, *Green Chem.*, 2017, **19**, 68–75.

23 J. Marcus, D. Touraud, S. Prévost, O. Diat, T. Zemb and W. Kunz, *Phys. Chem. Chem. Phys.*, 2015, **17**, 32528–38.

24 S. Prevost, T. Lopian, M. Pleines, O. Diat and T. Zemb, *J. Appl. Crystallogr.*, 2016, **49**, 2063–2072.

25 S. Shimizu and N. Matubayasi, *Phys. Chem. Chem. Phys.*, 2017, **19**, 26734–26742.

26 C. Lupis, *Chemical Thermodynamics of Materials*, North Holland, Dortrecht, 1983.

27 I. Prigogine and R. Defay, *Chemical Thermodynamics*, Longmans, London, 1954.

28 D. Gazzillo, *Mol. Phys.*, 1994, **83**, 1171–1190.

29 A. B. Bhatia and D. E. Thornton, *Phys. Rev. B*, 1970, **2**, 3004–3012.

30 K. Nishikawa, *Chem. Phys. Lett.*, 1986, **132**, 50–54.

31 H. Hayashi, K. Nishikawa and T. Iijima, *J. Appl. Crystallogr.*, 1990, **23**, 134–135.

32 D. J. Struik, *Lectures on Classical Differential Geometry*, Addison-Wesley, Reading, Mass, 1961.

33 V. I. Smirnov, *A Course of Higher Mathematics. Volume III/1*, Pergamon Press, Oxford, 1964, vol. 2.

34 A. Marcilla, M. D. Serrano, J. A. Reyes-Labarta and M. M. Olaya, *Ind. Eng. Chem. Res.*, 2012, **51**, 5098–5102.

35 B. L. Beegle, M. Modell and R. C. Reid, *AIChE J.*, 1974, **20**, 1194–1200.

36 R. C. Reid and B. L. Beegle, *AIChE J.*, 1977, **23**, 726–732.

37 T. C. Boberg and R. R. White, *Ind. Eng. Chem. Fundam.*, 1962, **1**, 40–45.

38 J. G. Kirkwood and F. P. Buff, *J. Chem. Phys.*, 1951, **19**, 774–777.

39 D. G. Hall, *Trans. Faraday Soc.*, 1971, **67**, 2516–2524.

40 A. Ben-Naim, *J. Chem. Phys.*, 1977, **67**, 4884–4890.

41 E. Matteoli and L. Lepori, *J. Chem. Phys.*, 1984, **80**, 2856–2863.

42 J. P. O'Connell, *Fluid Phase Equilib.*, 1993, **83**, 233–242.

43 S. Shimizu, *Proc. Natl. Acad. Sci. U. S. A.*, 2004, **101**, 1195–1199.

44 S. Shimizu and C. L. Boon, *J. Chem. Phys.*, 2004, **121**, 9147–9155.

45 A. Perera, R. Mazighi and B. Kežić, *J. Chem. Phys.*, 2012, **136**, 174516.

46 B. Kežić and A. Perera, *J. Chem. Phys.*, 2012, **137**, 134502.

47 P. E. Smith, E. Matteoli and J. P. O'Connell, *Fluctuation theory of solutions : Applications in chemistry, chemical engineering, and biophysics*, CRC Press, Boca Raton, FL, 2013.

48 S. Shimizu and N. Matubayasi, *J. Phys. Chem. B*, 2014, **118**, 3922–3930.

49 S. Shimizu and N. Matubayasi, *Phys. A Stat. Mech. its Appl.*, 2018, **492**, 1988–1996.

50 D. T. Bowron, J. L. Finney, A. Hallbrucker, I. Kohl, T. Loerting, E. Mayer and A. K. Soper, *J. Chem. Phys.*, 2006, **125**, 1–14.

51 P. Saurel, *Ann. Math.*, 1904, **5**, 188–202.

52 J. W. Gibbs, *Trans. Conn. Acad. Arts Sci.*, 1876, **3**, 198–248.

53 D. J. Korteweg, *Arch. Néerl. Sci. Exact. Nat.*, 1890, **24**, 58–98.

54 D. J. Korteweg, *Arch. Néerl. Sci. Exact. Nat.*, 1891, **24**, 295–368.

55 J. M. H. Levelt Sengers, *How Fluids Unmix : Discoveries by the School of van der Waals and Kamerlingh Onnes*, Koninklijke Nerlandse Akademie van Wetenschappen, Amsterdam, 2002.

56 R. M. Mazo, *J. Chem. Phys.*, 2008, **129**, 154101.

57 P. E. Smith, *J. Chem. Phys.*, 2008, **129**, 124509.

58 M. Kang and P. E. Smith, *J. Chem. Phys.*, 2008, **128**, 244511.

59 J. G. Kirkwood and F. P. Buff, *J. Chem. Phys.*, 1951, **19**, 774–777.

60 B. Widom, *J. Chem. Phys.*, 1967, **46**, 3324–3333.

61 N. W. Ashcroft and D. C. Langreth, *Phys. Rev.*, 1967, **156**, 685–692.

62 K. Hoshino, *J. Phys. F Met. Phys.*, 1983, **13**, 1981–1992.

63 V. I. Smirnov, *A Course of Higher Mathematics, Volume II*, Pergamon Press, Oxford, 1964.

64 R. Cortes-Huerto, K. Kremer and R. Potestio, *J. Chem. Phys.*, 2016, **145**, 141103.

Figures

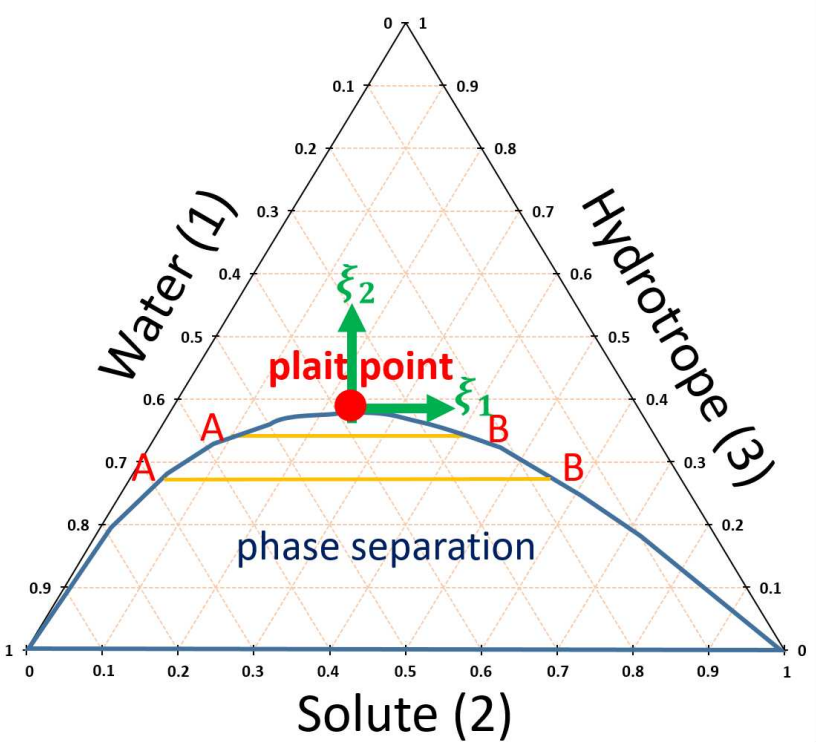

Figure 1. A schematic representation of a ternary phase diagram. The plait point is where the two end points (A and B) of the tie line (orange) merges into a single point. The principal axes have been indicated in green.

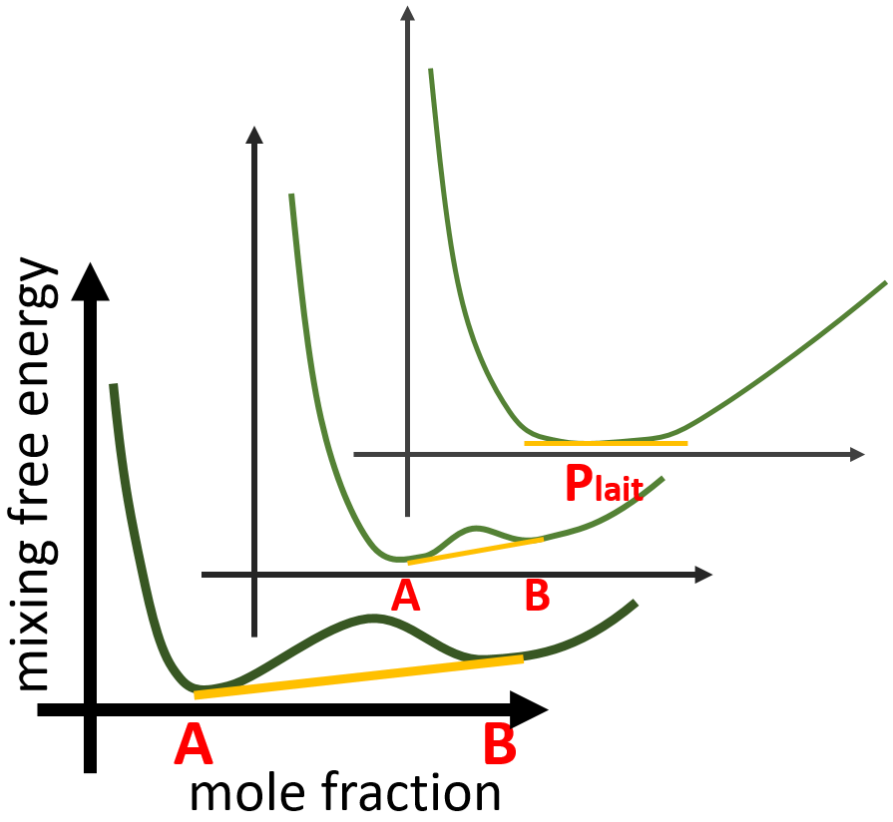

Figure 2. A schematic diagram showing the mixing free energy (g_{mix}) along the tie line direction (orange). The end points A and B gets closer towards the plait point, at which the two points merge into a single point.

Table of contents graphics